05,13

Surface magnetostatic spin waves in bilayer periodic structures YIG/GaAs

© A.A. Martyshkin[1,2], K. Bublikov[3], A.V. Sadovnikov[1,2]

[1] Saratov National Research State University,
Saratov, Russia
[2] Far Eastern Federal University,
Vladivostok, Russia
[3] Slovak University of Technology,
84104 Bratislava, Slovakia

E-mail: aamartyshkin@gmail.com

Received June 29, 2023
Revised November 7, 2023
Accepted November 8, 2023

We investigated spin waves (SW) propagation in a ferromagnetic/semiconductor array of parallel semiconductor strips of gallium arsenide (GaAs) placed on the surface of a ferromagnetic film of iron-yttrium garnet (YIG). Used by numerical simulation investigated SWs properties propagating in the tangentially magnetized YIG/GaAs structure. The effect of controlled nonreciprocity of the spin-wave signal, manifested in the change of the longitudinal wave number at variation of the concentration of electron density in GaAs strips, has been demonstrated. The influence of the concentration of electron density in an array of GaAs strips on the properties of SWs propagating in a ferrite film has been studied in the case when the Bragg resonance condition is satisfied for transverse wave numbers. The proposed structure can be applied to signal processing devices based on magnonics principles.

Keywords: spin waves, heterostructures, ferromagnetic, nonreciprocity.

DOI: 10.61011/PSS.2023.12.57690.132

1. Introduction

Magnonics is one of the possible directions for overcoming the limitations of traditional microelectronics based on complementary metal-oxide-semiconductor (CMOS) [1]. One of the ways to overcome the limitations of CMOS technologies is the use of structured thin-film magnetic spin-waveguide structures [2,3]. At the present stage of the magnonics development, we are talking about the design of components that can be combined as independent units into magnonic networks [4–6] to obtain functional devices for encoding, transmitting and processing information.

Spin-wave transport in bilayer ferromagnetic/semiconductor structures is of great interest [7–9]. It is known that metallization of the ferrite layer results in the appearance of non-reciprocal SW properties, manifested in the transformation of dispersion characteristics when the SW direction changes to the opposite [10]. The semiconductor layer on the surface of a ferromagnetic film is similar to a metal layer on the ferromagnetic film [11], and is accompanied by a change in the dispersion and transmission spectra of SW, as well as the appearance of nonreciprocal effects [7]. In the paper [12] it was shown that free charge carriers optically injected into the semiconductor layer make it possible to control the dispersion characteristics and transmission spectra of SW.

Interest in semiconductor/ferromagnetic heterostructures in recent years is due to the development of methods for manufacturing the laser radiation controlled nanoscale structures [13], as well as studies that solved the problem of growing thin structured ferromagnetic films on semiconductor substrates [14]. The bilayer structures consisting of a film of yttrium iron garnet (YIG) grown on a substrate of gallium arsenide (GaAs) [15] of particular interest due to the extra low attenuation of spin waves in YIG films [16]. The presence of many ways to change the rate of injection and recombination of free charge carriers in ferrite/semiconductor heterostructures makes it possible to create reconfigurable devices based on magnon principles [17]. For example, based on the effect of laser radiation induced changes in the conductivity of the GaAs layer in the YIG/GaAs structure, it seems possible to create controlled magnonic devices that can be integrated with CMOS technologies. At the same time, the use of magnon crystals (MCs), which are media with periodic changes in parameters affecting the SW propagation, makes it possible to observe nonreciprocal effects manifested in changes in the SW spectra and spatial distributions of the SW field amplitude, for example, in a thin permalloy film with nickel stripes on it surface [18].

A general analytical approach to the study of SW transport in bilayer semiconductor/ferromagnet structures is the solution of the electromagnetic problem based on Maxwell's equations [11]. The effect of the semiconductor layer on SWs propagating in the ferromagnetic layer is described by the influence of free charge carriers in the solid body, complying with the Boltzmann kinetic equation of motion [11,19,20]. The dynamics of the ferromagnet magnetization can be described by solving the Landau–Lifshitz equation of motion in the time domain. However, for cases

when the internal magnetic field of the ferromagnet is quasi-static and quasi-homogeneous, the problem can be reduced to the linearized solution of the Landau–Lifshitz equation with a gyrotropic permeability tensor [11]. In the general case, for structures containing gyrotropic materials, the Maxwell's equation solution does not split into independent magnetic and electric waves (H- and E-type) [11]. This results in the need to use numerical methods for analyzing the magnon structures in the electrodynamic approach, for example, the finite element method (FEM) [21].

This paper relates to a numerical electrodynamic analysis of the exchangeless propagation of SW in structure consisting of an array of GaAs strips located on the surface of YIG layer. It is shown that when the concentration changes of free charge carriers in semiconductor strips of the YIG/GaAs structure, the band gaps for SW propagation are formed in the spectrum, which is similar to the case of the band gaps formation in magnon-crystalline structures. The proposed structure can serve in magnon integrated circuits as a spatial-frequency signal filter tunable by laser radiation.

2. Structure under study and numerical model

The type of two-dimensional calculation cell for the bilayer structure under study is presented in Figure 1. GaAs strips are deposited parallel to each other on the YIG layer through a buffer layer AlO_x $2\,\mu$m thick. The buffer layer AlO_x is used to ensure the compatibility of different crystal structures of YIG and GaAs in the fabrication of the YIG/GaAs heterostructure [7,15]. The thickness of the YIG film is $10\,\mu$m. GaAs strips are $1\,\mu$m thick and $50\,\mu$m wide. In the model under study, the structure is presented as infinite and homogeneous along the axis z and periodic (with a period $D = 200\,\mu$m) along the axis x. The structure was magnetized tangentially along the axis x by a magnetic field $|\mathbf{H}| = 1308$ Oe, which provided the possibility of SW propagation along the axis z with a longitudinal wave number $\mathbf{k}_{||}$ in the Damon–Eschbach (DE) configuration [22]. The selected configuration of the structure and magnetic field makes it possible to excite SWs propagating through the structure both in the positive direction along the axis z ($\mathbf{k}_{||}^{+}$) when $\mathbf{k}_{||} \uparrow\uparrow z$, and in the negative direction along the axis z ($\mathbf{k}_{||}^{-}$) when $\mathbf{k}_{||} \uparrow\downarrow z$. SW propagation at an angle different from 90° relative to the external magnetization field results in the appearance of a wave vector component ($\mathbf{k}_{\perp}$) directed along the axis x. For plane waves the presence of the component $\mathbf{k}_{\perp}$ means that SW propagation through the structure occurs at angles to the magnetizing magnetic field other than the perpendicular orientation, and in this case the wave number can be represented as

$$\mathbf{k} = \mathbf{k}_{||} + \mathbf{k}_{\perp}. \qquad (1)$$

The numerical model of the structure under study is presented in the form of a two-dimensional cell of one

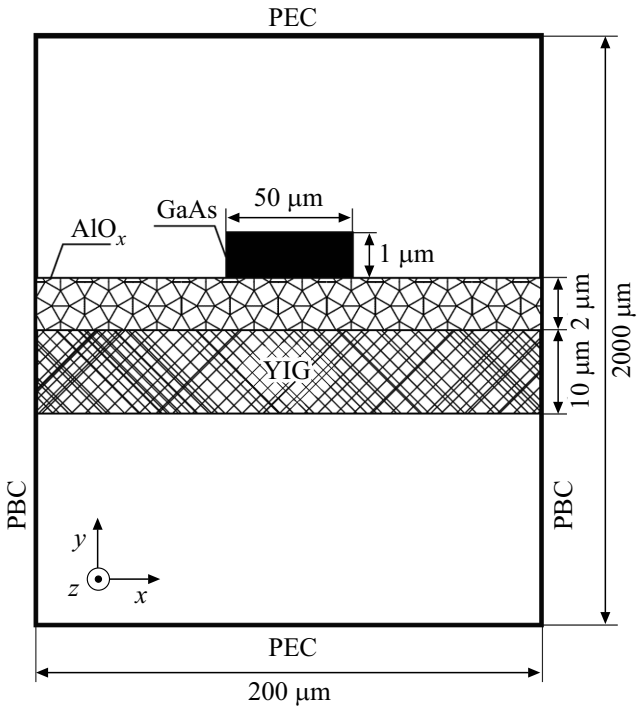

Figure 1. Schematic representation of cell of one period of structure under study during numerical simulation.

period of the structure along the direction of the axis x (1). Periodic boundary conditions (PBC) were imposed on the left and right boundaries of the computational cell, and a perfect electric conductor (PEC) was used as the boundary conditions for the upper and lower boundaries. Note here that the distance at which the PEC was installed corresponded to the convergence of all in question eigenmode solutions of SW.

The material parameters were set as follows. For YIG layer the saturation magnetization $M_S = 1.39 \cdot 10^5$ G, $\gamma = 2.8$ MHz/Oe, dielectric constant $\epsilon = 12.7$. For layer AlO_x: dielectric constant $\epsilon = 9$ [23]. For GaAs: average electron collision frequency $\nu_e = 0.05$ GHz, effective electron mass $m_e = 10^{-32}$ kg, crystal dielectric constant $\epsilon_d = 12.9$, electron charge $q_e = 1.6 \cdot 10^{-19}$ C [24]; electron density $N_e$was considered as a control parameter.

To calculate the natural modes of electromagnetic waves (EMW) of the computational cell, the method described in [21] was used. The Helmholtz wave equation for the electric field vector $\mathbf{E}$ [25] was solved using the finite element method:

$$V \times (\mu^{-1} V \times \mathbf{E}) - \frac{2\pi f^2}{c_0^2}\left(\epsilon - \frac{i\sigma}{2\pi f \epsilon_0}\right)\mathbf{E} = 0, \qquad (2)$$

where f — frequency of the natural mode of the wave, ϵ_0 — dielectric constant of vacuum, c_0 — speed of light in vacuum. Coordinate-dependent material properties in equation (2): μ — relative magnetic permeability, ϵ — relative dielectric constant and σ — conductivity. Solving the problem of searching for eigenmodes using the

Bloch form of the wave solution for $E(x, y)$ equation (2) and applying boundary conditions, one can obtain $k_z \equiv k$ eigenvalues for given frequencies f. For the structure under study, the in question form of the wave solution is a quasi-H type EMW [26], while the magnetic permeability tensor $\hat{\mu}$, which describes the gyromagnetic properties of YIG to take into account the exchangeless nature of SW, has the form

$$\hat{\mu} = \begin{bmatrix} 1 & 0 & 0 \\ 0 & \mu(f) & i\mu_a(f) \\ 0 & -i\mu_a(f) & \mu(f) \end{bmatrix}, \qquad (3)$$

$$\mu(f) = \frac{f_H(f_H + f_M) - f^2}{f_H^2 - f^2}, \ \mu_a(f) = \frac{f_M f}{f_H^2 - f^2}, \qquad (4)$$

where $f_M = 4\gamma\pi M_s = 3.8\,\text{GHz}$, $f_H = \gamma H_0 = 3.662\,\text{GHz}$. This approach to describing the magnetic properties of solids is valid for quasi-uniformly magnetized thin films and layers without dividing the spatial magnetization into domains, and without the possibility of remagnetization. The dielectric constant tensor described in the papers [11,19,20] makes it possible to take into account the gyroelectric properties of the semiconductor and SW interaction with GaAs electrons. It is assumed that electrons inside GaAs (hole charge carriers were not taken into account) comply with the Boltzmann kinetic equation of motion in the hydrodynamic approximation.

3. Distribution of spin waves in structure Y(IG/GaAs

Let's discuss the case when SWs distribute along GaAs strips ($\mathbf{k} \parallel z$), ay yjay only longitudinal component $\mathbf{k} \equiv \mathbf{k}_\parallel$ is considered). According to papers [7,27,28] one can suppose that our structure is similar to partially metallized magnetic layer. The conductive non-magnetic layer will act on SW dissipation by shielding with electromagnetic field induction, reducing the penetration depth in comparison with SW propagation through magnetic film [28,29]. According to [11], in the case of complete metallization of the magnetic film from the side of the EMW maximum the upper limit of SW frequency for the case $k \to \infty$ shifts from the extreme value $f_H + f_M/2$ to $f_H + f_M$. For intermediate cases, with wave number increasing, the maximum wave frequency would reach a position between the values $f_H + f_M/2$ and $f_H + f_M$. In the general case, for waves with $\mathbf{k}_\parallel^+$ the maximum frequency of the dispersion dependence of SW (in the interval between $f_H + f_M/2$ and $f_H + f_M$) will depend on the width and the thickness of GaAs strips, and also on the properties of GaAs material: average collision frequency, effective electron mass and electron charge concentration, then by fixing all parameters except the electron charge concentration, by varying N_e one can control SW dispersion curve between limiting cases of „YIG film" and „YIG layer with ideal electrically conductive strips".

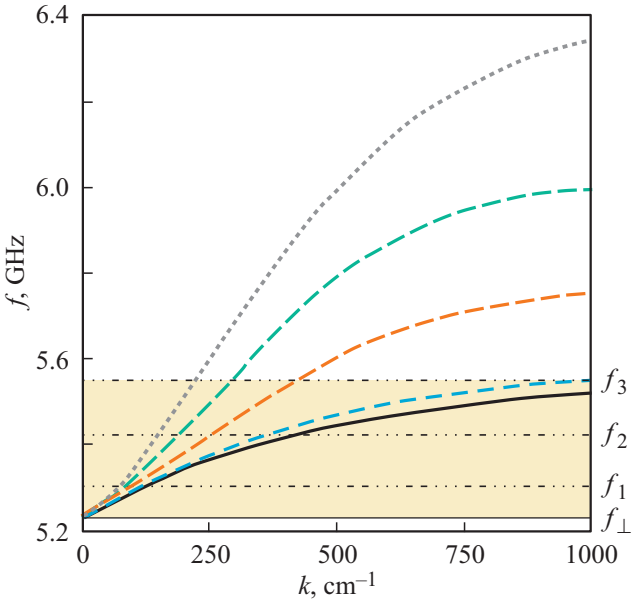

Figure 2. Dispersion characteristics of SWs propagating along the direction z ($\mathbf{k}_\parallel^+$) of YIG film without GaAs strips (solid curve), in the case of GaAs stripes replacement with PEC (dashed curve), and at different electron concentrations in GaAs strips: $N_e = 5 \cdot 10^{16}\,\text{cm}^{-3}$ (blue dashed curve), $N_e = 2.5 \cdot 10^{17}\,\text{cm}^{-3}$ (orange dashed curve) and $N_e = 1 \cdot 10^{18}\,\text{cm}^{-3}$ (green dashed curve). The frequency band of exchangeless SWs is highlighted with the yellow region (with the limits of ferromagnetic resonance in a tangentially magnetized ferromagnetic layer f_0 and $f_H + f_M/2$). $f_1 = 5.3\,\text{GHz}$, $f_2 = 5.425\,\text{GHz}$ and $f_3 = 5.55\,\text{GHz}$ indicate the frequencies at which the various parameters were simulated.

The results of simulation of the dispersion dependences of SW with $\mathbf{k}_\parallel^+$ for YIG film without an array of GaAs strips (solid curve) and for the structure under study with strips of an ideal electrical conductor (dashed curve) are shown in Figure 2. Since the simulated YIG layer is homogeneous and infinite along the axes x and z, the resulting dispersion curve for YIG film without the array of GaAs strips coincides with the dispersion of DE mode [22]. The yellow area in Figure 2 marks the SW band with the already mentioned upper limit $f_H + f_M/2$, and the lower limit $f_0 = \sqrt{f_H(f_H + f_M)}$ with frequency coinciding with the magnitude of ferromagnetic resonance in tangentially magnetized ferromagnetic layer [30]. Figure 2 shows the result of simulating SW dispersion relations for waves with $\mathbf{k}_\parallel^+$ at different electron concentrations ($N_e = 5 \cdot 10^{16}\,\text{cm}^{-3}$ blue curve, $N_e = 2.5 \cdot 10^{17}\,\text{cm}^{-3}$orange curve and $N_e = 1 \cdot 10^{18}\,\text{cm}^{-3}$ green curve) in the GaAs lateral strips array. An increase in free charge carriers results in increase in the maximum SW frequency. At the same time, the values of SW group velocities in the range of wave numbers below the frequency maximum increase with increase in concentration of free charge carriers N_e in GaAs.

Note that for the case when at GaAS boundaries the boundary conditions of the type of electric wall of infinite

conductivity are established, the dispersion relations for SW $\mathbf{k}_{\|}^{-}$ do not coincide with the result of calculating the SW dispersion for the DE mode. At the same time, the resulting dispersion for the YIG film without GaAs strips (see Figure 2, solid curve) is identical. This result is consistent with the model of SW in magnetic films metallized on the side opposite to the maximum strength of the electromagnetic field induced by the wave [11]. The reason for such difference in the properties of SWs propagating with counter-directed wave vectors is the relation between the maximum of EMW components distribution and the mutual direction $\mathbf{k}$ and $\mathbf{H}$. For the structure under study the maximum of the EMW distribution with the mutual orientation $\mathbf{k}_{\|}^{-}$ falls on the surface of YIG layer facing the direction opposite to the array of GaAs strips. Thus, waves $\mathbf{k}_{\|}^{-}$ are weakly influenced by strips. This effect is called nonreciprocity [7,31] and for the structure under study will change with the change in electron concentration in GaAs.

The frequency range from f_0 to $f_H + f_M/2$ is of the greatest practical interest due to the possibility of SW excitation in YIG film without GaAs strips [32]. In this range at characteristic frequencies $f_1 = 5.3\,\text{GHz}$, $f_2 = 5.425\,\text{GHz}$ and $f_3 = 5.55\,\text{GHz}$, marked in Figure 2 by horizontal dash-dotted lines, the SW nonreciprocity parameter $\delta k_{\|,f} = k_{\|}^{-} - k_{\|}^{+}$ was obtained with change in the electron concentration in GaAs.

Figure 3, *a* shows the numerically calculated nonreciprocity parameter $\delta k_{\|,f} = k_{\|}^{-} - k_{\|}^{+}$, which shows the difference in wave numbers for counter-directed SWs at a given frequency. It can be seen that the value of the nonreciprocity parameter increases along with the values of both the electron concentration and the SW frequency. Spin waves with $\mathbf{k}_{\|}^{-}$ are practically unaffected by GaAs, which makes it impossible to determine the parameter $\delta k_{\|}$ outside the frequency band of the DE mode.

When SW propagates at an angle to the axis z (and therefore to GaAs strips), in other words, at angles different from 90° to the field direction H, the SW wave vector will contain both longitudinal and transverse components according to equation (1). In fact, the transition from the state $\mathbf{k} \perp \mathbf{H}$ to $\mathbf{k} \perp \mathbf{H}$ corresponds to the transition from the configuration of surface spin waves to the inverse bulk spin wave [11,31].

Due to the periodic nature of the structure under study, provided by the GaAs lattice, it is possible to fulfill the Bragg conditions $\mathbf{k}_{\text{B}} = \mathbf{k}_{\perp} = m\pi \div D$, where m — an integer. This condition specifies the relationship between the wave vector $\mathbf{k}_{\perp}$ (normally oriented to the lattice), the structure period D and the Bragg resonance order m. To study the formation of no-pass zones in the SW spectra for the structure under study as function of the electron concentration in the GaAs strips the isofrequency characteristics were obtained, Figure 4. For the structure model under study the isofrequencies represent the dependence of the longitudinal component of the wave number $k_{\|}$ on the transverse component of the wave number $k_{\perp}$ at

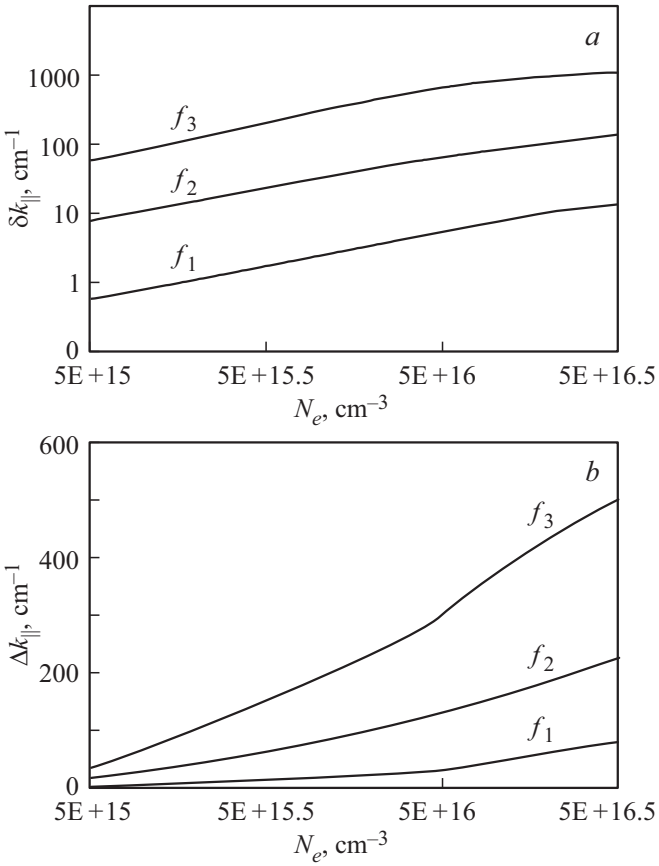

Figure 3. *a* — introduced nonreciprocity parameter $\delta k_{\|,f} = k_{\|}^{-} - k_{\|}^{+}$ vs. GaAs electron concentration, N_e, at frequencies $f_1 = 5.3\,\text{GHz}$, $f_2 = 5.425\,\text{GHz}$ and $f_3 = 5.55\,\text{GHz}$. *b* — the range of longitudinal wave numbers of the Bragg band gap $\Delta k_{\|}$ at a constant transverse wave number $(k_{\perp}D/\pi)$ was obtained as a function of electron concentration, N_e at frequencies $f_1 = 5.3\,\text{GHz}$, $f_2 = 5.425\,\text{GHz}$ and $f_3 = 5.55\,\text{GHz}$.

fixed frequency. Thus, each point of the isofrequency dependence is a vector $\mathbf{k} = \mathbf{k}_{\|} + \mathbf{k}_{\perp}$ at a given frequency. To simulate SW with a wave vector having non-zero transverse component, the longitudinal component of the wave number was estimated as a function of the given frequency and Floquet wave number, specified at periodic boundary conditions. The Floquet wave number determined the longitudinal component of the waves, and in the next step this value was normalized to the Brillouin zone $(k_{\perp}D/\pi)$. The obtained isofrequency dependences are presented for frequencies $f_1 = 5.3\,\text{GHz}$ (Figure 4, *a*) and $f_3 = 5.55\,\text{GHz}$ (Figure 4, *b*). Figure 4 shows the isofrequency dependences for YIG film without the array of GaAs strips (black curves), with the strips replaced by PEC (gray curves) and for different electron concentrations in GaAs strips $N_e = 5 \cdot 10^{16}\,\text{cm}^{-3}$ (blue curves) and $N_e = 2.5 \cdot 10^{17}\,\text{cm}^{-3}$ (orange curves).

Figure 4, *a* shows that in YIG film without GaAs strips SW can propagate in all directions due to the periodic lattice absence. The influence of the periodic lattice increases

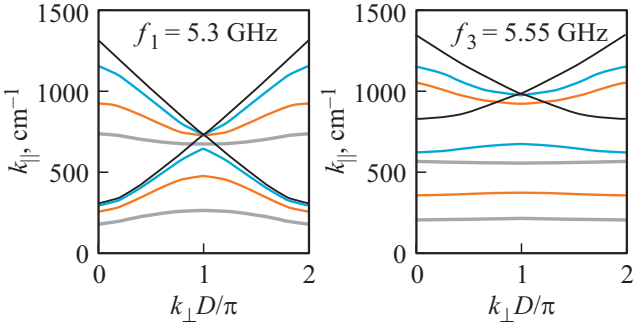

Figure 4. Isofrequency dependences $k_{\|}(k_{\perp})$ of SW in the structure under study are presented for frequencies $f_1 = 5.3$ GHz (a) and $f_3 = 5.55$ GHz (b). Both panels show isofrequency dependences for a pure YIG layer (black curves), for the structure under study with replacement of semiconductor strips by PEC (gray curves), as well as for the electron density of GaAs strips $N_e = 5 \cdot 10^{16}$ cm^{-3} (blue curves) and $N_e = 2.5 \cdot 10^{17}$ cm^{-3} (orange curves).

with increase in electron concentration in GaAs strips, which is accompanied by the appearance and increase of wave vectors band, at which SW transfer is impossible. The same trend is visible at the frequency $f_3 = 5.55$ GHz (see Figure 4, b), but the increase in the band gap for $k_{\|}$ wave numbers, along with the increase in the electron concentration in GaAs strips, has a non-monotonic nature.

To compare the frequency dependences of the band gap $\Delta k_{\|}$ (for wave number $k_{\|}$) on the GaAs electron concentration, simulation was carried out at $k_{\perp} = \pi/D$ for frequencies f_1, f_2 and f_3. The results $\Delta k_{\|}$ $(f, N_e, k_{\perp} = \pi/D)$ (Figure 3, b), show the increase in $\Delta k_{\|}$ as the electron concentration in GaAs increases, and the increase becomes stronger and non-monotonic with frequency increasing. The results obtained demonstrate the possibility of controlling the wavelengths of SW propagation in the structure under study by changing N_e. Note that the range of changes in the electron concentration in GaAs, in which change in the value $N_e$results in a significant change in $\Delta k_{\|}$ and is $5 \cdot 10^{15} \div 1 \cdot 10^{18}$ cm^{-3}. At the same time, the change in the component $k_{\perp}$ for $\Delta k_{\|}$ shows that control of the SW spectrum is possible in the structure under study.

In this paper, we analyzed the electrodynamic characteristics in the structure consisting of array of gallium arsenide strips on the surface of ferromagnetic film of yttrium iron garnet. The properties of SW propagating in the proposed structure are shown by electrodynamic problem solution using the finite element method. It is shown that the dispersion law for SW has limiting cases of free YIG layer and YIG/GaAs structure with the strip array replaced by an ideal electrical conductor. In this frequency band, the SW dispersion law can be modified by changing the number of free charge carriers in GaAs strips. At the same time, a nonreciprocity effect with increase in free charge carriers in the GaAs strips is observed between SWs with counter-directed **k**parallel to the GaAs strips. In an experiment, the change in the number of free carriers in semiconductor layer can be realized by the method of local laser irradiation [12]. Thus, the results obtained in this paper allow us to consider the structure under study as a spatial-frequency filter of spin-wave signals controlled by laser radiation.

Funding

The study was carried out with the support of the Ministry of Science and Higher Education of the Russian Federation for state support of scientific research conducted under the guidance of leading scientists in Russian higher educational institutions, scientific foundations and state research centers (project No. 075-15-2021-607).

Conflict of interest

The authors declare that they have no conflict of interest.

References

[1] S. Thompson. Int.Technol. J. (Q3): **19**, 1 (1998). ISSN 1535-766X
[2] V. Kruglyak, S. Demokritov, D. Grundler. Magnonics J. Physics D **43**, 264001 (2010).
[3] S.A. Nikitov, D.V. Kalyabi, I.V. Lisenkov, A.N. Slavin, Yu.N. Barabanenkov, S.A. Osokin, A.V. Sadovnikov, E.N. Beginin, M.A. Morozova, Yu.P. Sharaevsky, Yu.A. Filimonov, Yu.V. Khivintsev, S.L. Vysotsky, V.K. Sakharov, E.S. Pavlov. Usp. Fiz. Nauk **58**, 10 (2015).
[4] C.S. Davies, A. Francis, A.V. Sadovnikov, S.V. Chertopalov, M.T. Bryan, S.V. Grishin, D.A. Allwood, Y.P. Sharaevskii, S.A. Nikitov, V.V. Kruglyak. Phys. Rev. B **92**, 020408 (2015).
[5] E. Beginin, A. Sadovnikov, A.Y. Sharaevskaya, A. Stognij, S. Nikitov. Appl. Phys. Lett. **112**, 122404 (2018).
[6] A. Sadovnikov, E. Beginin, S. Odincov, S. Sheshukova, Y.P. Sharaevskii, A. Stognij, S. Nikitov. Appl. Phys. Lett. **108**, 172411 (2016).
[7] A.V. Sadovnikov, E.N. Beginin, S.E. Sheshukova, Y.P. Sharaevskii, A.I. Stognij, N.N. Novitski, V.K. Sakharov, Y.V. Khivintsev, S.A. Nikitov. Phys. Rev. B **99**, 054424 (2019).
[8] Yu.V. Gulyaev, S. Nikitov. FTT **25**, 2515 (1983). (in Russian).
[9] A. Kindyak. Mater. Lett. **24**, 359 (1995).
[10] R. De Wames, T. Wolfram. J. Appl. Phys. **41**, 5243 (1970).
[11] A. Gurevich, G. Melkov. Magnetization Oscillations and Waves. Taylor & Francis (1996).
[12] A. Sadovnikov, E. Beginin, S. Sheshukova, Y.P. Sharaevskii, A. Stognij, N. Novitski, V. Sakharov, Y.V. Khivintsev, S. Nikitov. Phys. Rev. B **99**, 054424 (2019).
[13] G. Gubbiotti. Three-Dimensional Magnonics. Jenny Stanford Publishing (2019).
[14] A. Stognij, L. Lutsev, N. Novitskii, A. Bespalov, O. Golikova, V. Ketsko, R. Gieniusz, A. Maziewski. J. Physics D **48**, 485002 (2015).
[15] L. Lutsev, A. Stognij, N. Novitskii, V. Bursian, A. Maziewski, R. Gieniusz. J. Physics D **51**, 355002 (2018).
[16] Kajiwara, K. Harii, S. Takahashi, J. Ohe, K. Uchida, M. Mizuguchi, H. Umezawa, H. Kawai, K. Ando, K. Takanashi, S. Maekawa, E. Saitoh. Nature **464**, 262 (2010).

[17] A. Barman, G. Gubbiotti, S. Ladak, A.O. Adeyeye, M. Krawczyk, J. Gräfe, C. Adelmann, S. Cotofana, A. Naeemi, V.I. Vasyuchka, B. Hillebrands, S.A. Nikitov, H. Yu, D. Grundler, A.V. Sadovnikov, A.A. Grachev, S.E. Sheshukova, J.-Y. Duquesne, M. Marangolo, G. Csaba, W. Porod, V.E. Demidov, S. Urazhdin, S.O. Demokritov, E. Albisetti, D. Petti, R. Bertacco, H. Schultheiss, V.V. Kruglyak, V.D. Poimanov, S. Sahoo, J. Sinha, H. Yang, M. Münzenberg, T. Moriyama, S. Mizukami, P. Landeros, R.A. Gallardo, G. Carlotti, J.-V. Kim, R.L. Stamps, R.E. Camley, B. Rana, Y. Otani, W. Yu, T. Yu, G.E.W. Bauer, C. Back, G.S. Uhrig, O.V. Dobrovolskiy, B. Budinska, H. Qin, S. van Dijken, A.V. Chumak, A. Khitun, D.E. Nikonov, I.A. Young, B.W. Zingsem, M. Winklhofer. J. Physics: Condens. Matter **33**, 413001 (2021).
[18] M. Mruczkiewicz, P. Graczyk, P. Lupo, A. Adeyeye, G. Gubbiotti, M. Krawczyk. Phys. Rev. B **96**, 104411 (2017).
[19] A. Gurevich. Magnetic resonance in ferrites and antiferromagnets. Nauka, M. (1973).
[20] F. Bass A. Bulgakov. Kinetic and Electrodynamic Phenomena in Classical and Quantum Semiconductor Superlattices. Nova Science Publishers (1997).
[21] D.M. Cook. The theory of the electromagnetic field. Englewood Cliffs (1975).
[22] R.W. Damon, J. Eshbach. J. Phys. Chem. Solids **19**, 308 (1961).
[23] W. Li, Z. Chen, R.N. Premnath, B. Kabius, O. Auciello. J. Appl. Phys. **110**, 024106 (2011).
[24] J. Blakemore. J. Appl. Phys. **53**, R123 (1982).
[25] COMSOL Multiphysics and COMSOL Multiphysics Modeling Guide, 5.3: Introduction to RF Module, Stockholm, Sweden: COMSOL AB (2017).
[26] A.V. Sadovnikov, K. Bublikov, E. Beginin, S. Sheshukova, Y.P. Sharaevskii, S.A. Nikitov. JETP Lett. **102**, 142 (2015).
[27] Y. Fetisov, A. Makovkin, V. Studenov. Optically controlled microwave magnetostatic wave transmission line, in International Topical Meeting on Microwave Photonics. MWP'96 Technical Digest. Satellite Workshop (Cat. No 96TH8153) (1996). P. 37–40.
[28] M. Mruczkiewicz, M. Krawczyk. J. Appl. Phys. **115**, 113909 (2014).
[29] H. van den Berg. IEEE Transact. Magn. **27**, 5480 (1991).
[30] C. Kittel. J. Phys. Rad. **12**, 291 (1951).
[31] A. Prabhakar, D.D. Stancil. Spin waves: Theory and applications **5**. Springer (2009).
[32] S.N. Bajpai. J. Appl. Phys. **58**, 910 (1985).

Translated by I.Mazurov